

Mechanisms of Dioxin Formation from the High-Temperature Oxidation of 2-Bromophenol

CATHERINE S. EVANS AND
BARRY DELLINGER*

Louisiana State University, Department of Chemistry,
Baton Rouge, Louisiana 70803

The homogeneous, gas-phase oxidative thermal degradation of 2-bromophenol was studied in a 1 cm i.d., fused silica flow reactor at a concentration of 88 ppm, reaction time of 2.0 s, over a temperature range from 300 to 1000 °C. Observed products in order of yield were dibenzo-*p*-dioxin (DD) > 4,6-dibromodibenzofuran (4,6-DBDF) > 4-monobromodibenzofuran (4-MCDF), dibenzofuran (DF), 1-monobromodibenzo-*p*-dioxin (1-MBDD), naphthalene, bromonaphthalene, 2,4-dibromophenol, 2,6-dibromophenol, phenol, bromobenzene, and benzene. This result is in contrast to the oxidation of 2-chlorophenol, where the major product is 4,6-dichlorodibenzofuran (4,6-DCDF). 4,6-DBDF was observed in high yields in contrast to our previous results for the pyrolysis of 2-bromophenol, where 4,6-DBDF was not detected. The increase in 4,6-DBDF yields is attributed to hydroxyl radical being the major chain carrier under oxidative conditions, which favors hydrogen-abstraction reactions that lead to formation of 4,6-DBDF. However, DD is still the highest yield product under oxidative conditions because of the relative ease of displacement of Br• in the ring-closure reaction.

Introduction

Over the past decade there has been an increase in concern over the risk of environmental exposure to brominated flame-retardant-containing materials (1, 2). Many of these materials, such as electronic or “E-wastes”, find their way to waste-treatment facilities where they are burned (3–7). They are also subject to thermal degradation during accidental fires (8). Because of their chemical composition and combustion inhibition properties, they are prone to forming products of incomplete combustion, including polybrominated dibenzo-*p*-dioxins and dibenzofurans (PBDD/Fs).

Previous research has indicated that the presence of bromine during the combustion of hazardous wastes increases the production of PBDD/Fs and well as polychlorinated dibenzo-*p*-dioxins and dibenzofurans (PCDD/Fs) and mixtures of brominated and chlorinated dibenzo-*p*-dioxins and dibenzofurans (PXDD/Fs) (2, 9). It has also been established that brominated phenols and brominated flame retardants, e.g., polybrominated biphenyl ethers (PBDEs), are known precursors to PBDD/Fs (2, 3, 10–12). More importantly, some studies have shown that brominated phenols form more PBDD/Fs than the analogous chlorinated phenols form PCDD/Fs (10, 13, 14). With this knowledge, it is important to note that the toxicity of the PBDD/Fs has been shown to be similar to the analogous PCDD/Fs (15, 16).

Previous works on the oxidation of chlorinated phenols under “slow combustion conditions” (i.e., $T = 300\text{--}600\text{ }^{\circ}\text{C}$, reaction times between 10 s and 10 min) have reported the formation of PCDFs as the major products (17–20). However, in our recently reported studies on the high-temperature pyrolysis of both 2-chlorophenol and 2-bromophenol we reported the formation of PCDDs (dibenzo-*p*-dioxin (DD) and 1-monochlorodibenzo-*p*-dioxin (1-MCDD) or 1-monobromodibenzo-*p*-dioxin (1-MBDD)) was favored over the formation of PCDFs (4,6-dichlorodibenzofuran (4,6-DCDF) or 4,6-dibromodibenzofuran (4,6-DBDF)) (14, 21). There is an apparent contradiction that suggests that molecular oxygen is playing a large role in the product distribution and PCDD/F ratio.

In this paper, the thermal degradation of 2-bromophenol under oxidative conditions is reported for a reaction time of 2.0 s over the temperature range from 300 to 1000 °C and we compare these results to the results from previous studies of the pyrolysis of 2-bromophenol (14) as well as oxidation and pyrolysis of 2-chlorophenol (22).

Experimental Section

All experiments were performed using a high-temperature flow reactor system referred to in the archival literature as the System for Thermal Diagnostic Studies (STDS). The detailed design has been published elsewhere (23). In short, the STDS consists of a high-temperature, 1 cm i.d., fused silica flow reactor equipped with an in-line Varian Saturn 2000 GC/MS. The flow reactor is housed inside a furnace located inside a Varian GC, where the temperatures surrounding the reactor are controlled. Pressure inside the reactor is also maintained at 1.00 ± 0.15 atm. Gas-phase products are cryogenically trapped at the head of the GC column in preparation for chemical analysis.

To maintain a constant concentration of 88 ppm, 2-monobromophenol (2-MBP) (Aldrich) was injected into a 20% O₂ in helium gas stream by a syringe pump through a vaporizer maintained at 280 °C. Gas-phase samples of 2-MBP then were swept by the 20% O₂ in helium flow through heated transfer lines (300 °C) into a 35 cm long, 1.0 cm id., fused silica tubular flow reactor where the temperature was maintained between 300 and 1000 °C in individual experiments. The 20% O₂ in helium flow rate was varied with temperature, so that the residence time within the reactor was held at 2.0 s. The unreacted 2-MBP and thermal degradation products were then swept through a heated transfer line to another Varian GC, where they were cryogenically trapped at the head of a CP-Sil 8 phase capillary column (30 m, 0.25 mm i.d., 0.25 μm film thickness). To separate the individual reaction products the column was temperature programmed from –60 to 300 °C at 15 °C/min. Detection and quantification of the products were obtained using a Varian Saturn Mass Spectrometer which was operated in the full-scan mode (40–650 amu) for the duration of the GC run. The length of each experimental run was approximately 45 min.

Product concentrations were calculated based on the calibrations with standards of the products (Aldrich and Cambridge Isotope Lab) and the peak area counts from the chromatogram. The yields of the products were calculated using the expression

$$\text{yield} = \{[\text{product}]/[2\text{-MBP}]_0\} \times 100$$

where [product] is the concentration of the particular product formed (in moles) and [2-MBP]₀ is the initial concentration

* Corresponding author phone: (225) 578-6759; fax: (225) 578-3458; e-mail: barryd@lsu.edu.

TABLE 1. Percent Yield of Products of Gas-Phase Oxidation of 2-Bromophenol^a

product	temp (°C)											
	350	400	450	500	550	600	650	700	750	800	850	900
2-bromophenol	99.2	74.7	69.3	66.9	54.7	36.2	16.7	4.07	1.90	1.09	0.22	0.06
dibenzo- <i>p</i> -dioxin		1.36	3.27	12.6	22.2	17.0	16.6	8.01	3.30	0.18	0.12	
1-bromodibenzo- <i>p</i> -dioxin		0.04	0.08	0.13	0.15	0.12	0.07	0.06	0.03	0.02		
dibenzofuran					0.02	0.16	0.90	0.64	0.11	0.05		
4-bromodibenzofuran			0.06	0.22	0.52	0.58	0.82	0.46	0.17	0.10	0.005	
4,6-dibromodibenzofuran			0.46	1.14	1.69	1.89	2.40	1.25	0.22	0.11		
naphthalene		0.04	0.07	0.08	0.06	0.04	0.08	0.06	0.03	0.02	0.02	0.02
1-bromonaphthalene						0.04	0.10	0.06				
phenol						0.37	0.61					
2,4-dibromophenol		0.008	0.04	0.06	0.07	0.04	0.03	0.03	0.03	0.03	0.01	0.006
2,6-dibromophenol		0.03	0.11	0.10	0.17	0.04	0.03	0.01	0.007	0.005		
benzene						0.002	0.02	0.02				
bromobenzene						0.005	0.02	0.02	0.005	0.004	0.03	0.06
phenylethyne							0.007	0.005				

^a Percent yield = {[product]/[2-MBP]₀} × 100.

of 2-MBP (in moles) injected into the reactor. Multiple runs were performed for each temperature to ensure the repeatability of the experiments. Once the experimental procedure was fully developed, the repeatability of the experiments was within 10%.

Products (other than PBDD/Fs) were identified based on the NIST mass spectral library as well as the GC retention times and mass spectra of the standards for each product. Product concentrations were calculated based on the calibrations with standards of the products (Aldrich and Cambridge Isotope Lab) and the peak area counts from the chromatogram.

Standards for PBDD/Fs with less than four bromines were not available. Concentrations of observed PBDD/Fs are reported based on calibrations for the analogous PCDD/F. This is a reasonably accurate approach as the peak area counts for various chlorinated and brominated aromatics and PCDD/Fs and PBDD/Fs were compared, and it was found that the difference in calibration factors for brominated aromatic hydrocarbons and chlorinated aromatic hydrocarbons varied less than 10%.

Only three chromatographic peaks were observed that were tentatively identified as PBDD/F based on their mass spectra: 1-bromodibenzo-*p*-dioxin, 4,6-dibromodibenzofuran, and 4-bromodibenzofuran. The mass spectral library match qualities for each of these species were 264, 326, and, 248, respectively. These products are the same three PBDD/Fs that were anticipated based on the predicted pathways from previous research on formation of PCDD/F from the analogous 2-chlorophenol (22). In the 2-chlorophenol study the PCDD/F standards were available to confirm the identifications based on GC retention time and mass spectral pattern. Although standards were not available to confirm the identifications of PBDD/F, we are confident in the assignments based on the following: combination of mechanistically anticipated product formation; comparison of GC retention times, mass spectral response, and mass spectral patterns of chlorinated and brominated hydrocarbons; and previous studies of the formation of PCDD/F from 2-chlorophenol (22).

The heats of reaction, ΔH_{rxn} , for key steps in product formation pathways were calculated using AM1, semiempirical molecular orbital formalism. The calculations were performed using the MOPAC computation program that is contained within the ChemBats3D Pro computer application (24). Without experimental benchmarks the calculated ΔH_{rxn} cannot be considered to be completely accurate. They are shown to assess the likelihood of potential parallel pathways.

Pseudo-equilibrium calculations were performed to estimate the concentrations of reactive species such as •OH,

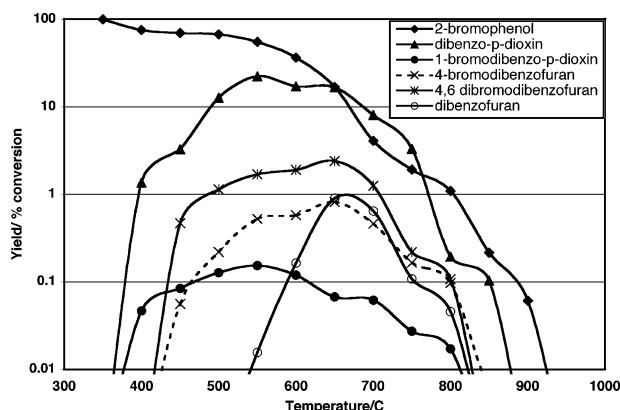


FIGURE 1. "Dioxin" products from the gas-phase oxidation of 2-MBP. [2-MBP]₀ = 88 ppm in helium. Gas-phase reaction time of 2.0 s.

O•, H•, and Br•. The Chemkin Equil code was used to calculate the concentrations of these species over a range of reaction temperature from 300 to 1000 °C (25). The initial inputs for the calculations were the same as the experimental runs in that the initial 2-MBP concentration was held at 88 ppm and the initial O₂ concentration was held at 20%. Over this temperature range the major molecular species are CO₂, H₂O, HBr, and Br₂. Other species of interest included in the calculation were •OH, O•, H•, Br•, HO₂, H₂, and CO.

Results

The temperature dependence of the oxidative thermal degradation of 2-MBP and the yield of "dioxin" products are presented in Figure 1 and Table 1 for a reaction time of 2.0 s. The non-dioxin products are presented in Figure 2 and Table 1. Figures 1 and 2 are presented on a semilogarithmic scale in which the percent yields of products (or percent yield of unconverted 2-MBP) are presented on a logarithmic scale versus temperature. The thermal degradation of 2-MBP initially increased gradually from 350 to 600 °C, achieving 99% destruction at 800 °C.

The predicted PBDD/F products, dibenzo-*p*-dioxin (DD), 1-bromodibenzo-*p*-dioxin (1-MBDD), and 4,6-dibromodibenzofuran (4,6-DBDF), were all observed for the oxidation of 2-MBP (cf. Figure 1 and Table 1). Other detected PBDD/F products were 4-bromodibenzofuran (4-MBDF) and dibenzofuran (DF). The two PBDD products, DD and 1-MBDD, were observed between 400 and 850 °C, reaching maximum yields of 22.2% and 0.15% at 550 °C, respectively. 4,6-DBDF and 4-MBDF were detected between 450 and 850 °C, reaching maximum yields at 650 °C of 2.40% and 0.82%, respectively.

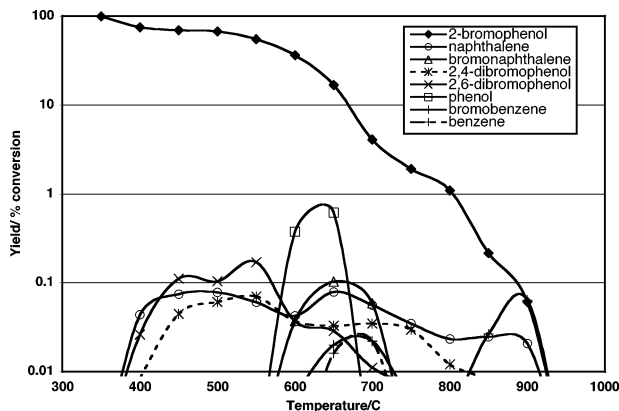


FIGURE 2. "Non-dioxin" products from the gas-phase oxidation of 2-MBP. [2-MBP]₀ = 88 ppm in helium. Gas-phase reaction time of 2.0 s.

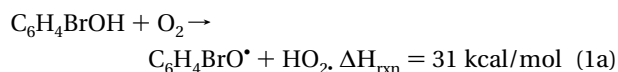
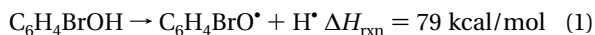
The final product, DF, was not detected until 550 °C and achieved a maximum yield of 0.90% at 650 °C. No brominated dioxin products were detected above 900 °C.

Non-PBDD/F products were also detected for the oxidation of 2-MBP (cf. Figure 2 and Table 1). Initially, at 400 °C 2,4-dibromophenol, 2,6-dibromophenol, and naphthalene were observed. 2,4-Dibromophenol and 2,6-dibromophenol achieved maximum yields of 0.07% and 0.17% at 550 °C, respectively. Naphthalene remained at a relatively constant yield from 400 to 700 °C and then decreased in yield at 900 °C, where it was no longer detected. Phenol, benzene, and phenylethyne were detected between 550 and 750 °C, achieving their respective maximum yields of 0.61%, 0.02%, and 0.007% at 650 °C. Bromobenzene was observed between 550 and 750 and 825–925 °C with local maximum yields of 0.02% at 650 °C and 0.06% at 900 °C.

Discussion

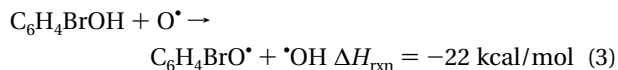
The formation of dioxin products (DD, 1-MBDD, and 4,6-DBDF) indicates that stable phenoxy radicals are formed in significant yields through loss of the hydroxyl hydrogen. The formation of aromatics (phenol, bromobenzene, and benzene) indicates that simple substitution reactions are occurring. The formation of 2,4-dibromophenol and 2,6-dibromophenol indicate evidence of bromination of 2-MBP. The formation of larger aromatic molecules at low temperatures (naphthalene and bromonaphthalene) is the result of reactions involving the release of CO from the phenoxy and bromophenoxy radicals that will then recombine to form naphthalene and bromonaphthalene.

2-MBP Decomposition. The addition of oxidative destruction pathways with the addition of molecular oxygen results in the decomposition of 2-MBP initiating at 600 °C rather than 650 °C, the temperature observed under pyrolytic conditions (14). The decomposition of 2-MBP can, in principle, be initiated by loss of the phenoxy hydrogen by unimolecular, bimolecular, or possibly other low-energy pathways (including heterogeneous reactions). Unimolecular decomposition of the oxygen–hydrogen bond (eq 1) is rapid with a reported rate coefficient for phenol of $k_1(430\text{--}930\text{ °C}) = 3.2 \times 10^{15} \exp(-86\,500/RT) \text{ s}^{-1}$ (26, 27). The direct bimolecular reaction with O₂ via reaction 1a is endothermic by 28 kcal/mol and viable only as minor initiation reaction



Bimolecular propagation reactions under oxidative conditions include attack by H[•], Br[•], [•]OH, and O[•]. In our previous

paper on the thermal degradation of 2-MBP under pyrolytic condition, ΔH_{rxn} for reactions with H[•] and Br[•] was discussed (14). It was determined that the most favorable reactions for generating the bromophenoxy radical were the abstraction of hydrogen by H[•] or Br[•]. With the addition of O₂ one can easily generate [•]OH and O[•] that can also abstract hydrogen via highly exothermic reactions (eqs 2 and 3)



Rate coefficients based on analogous reactions with phenol for eqs 2 and 3 are $k_2(1000\text{--}1150\text{ K}) = 6.0 \times 10^{12} \text{ cm}^3/\text{mol}/\text{s}$ (28) and $k_3(340\text{--}870\text{ K}) = 1.28 \times 10^{13} \exp(-2900/RT) \text{ cm}^3/\text{mol}/\text{s}$ (28). We used equilibrium calculations and other formalisms from the literature to estimate the [•]OH and O[•] concentration in our system (26, 28). Using these concentrations and the rate expressions given above (using $E_a(\text{eq } 1) = \Delta H_{\text{rxn}} = 79 \text{ kcal/mol}$), the rate of eq 2 is $\sim 200\times$ faster than eq 3 and a factor of 30 faster than eq 1. Thus, eq 2 is the dominant source of phenoxy radical under oxidative conditions.

Formation of Phenol, Bromobenzene, Benzene, 2,4-Dibromophenol, and 2,6-Dibromophenol. The formation of phenol is likely due to the exothermic displacement of bromine by H[•] ($\Delta H_{\text{rxn}} = -29 \text{ kcal/mol}$). The temperature range at which phenol is detected is much lower than for previous results of 2-MBP under pyrolytic conditions (14). This is due to the early onset of reaction of 2-MBP under oxidative conditions and the oxidation of phenol at higher temperatures.

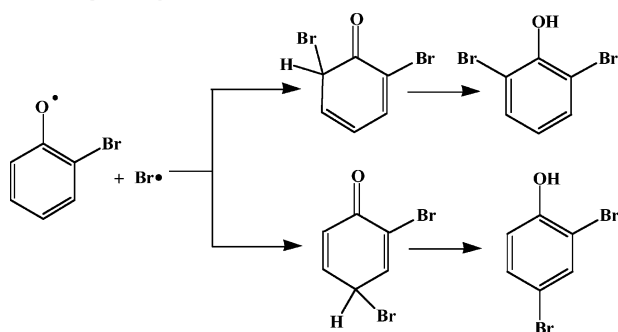
This result is very similar to that observed for pyrolysis and oxidation of 2-MCP (17, 22). The yield of phenol for the oxidation of 2-MBP is slightly higher than the yield for 2-MCP, which reflects the relative ease of bromine displacement compared to chlorine displacement due to the 15.5 kcal/mol lower carbon–bromine bond energy (29).

Bromobenzene and benzene are formed with much lower yields than phenol. These lower yields are due to the slightly endothermic displacements of hydroxyl by H[•] to form bromobenzene ($\Delta H_{\text{rxn}} = 2 \text{ kcal/mol}$) and hydroxyl from phenol by H[•] to form benzene ($\Delta H_{\text{rxn}} = 4 \text{ kcal/mol}$). However, bromobenzene reaches a maximum at 650 and 900 °C. The lower temperature maximum is due to the displacement of hydroxyl from 2-MBP by H[•]. The higher temperature maximum of bromobenzene is due to well-documented molecular growth pathways resulting from fragmentation of 2-MBP into C₂ species (30–32).

2,4-Dibromophenol and 2,6-dibromophenol are produced from bromination of the 2-MBP. Since displacement of hydrogen by Br[•] is endothermic, the direct reaction of Br[•] with 2-MBP is unlikely. The formation of dibromophenol is instead due to recombination of phenoxy radicals and Br[•]. Scheme 1 depicts the formation of 2,4-dibromophenol and 2,6-dibromophenol by Br[•] attack at the resonance-stabilized, *ortho*- or *para*-carbon sites of the bromophenoxy radicals ($\Delta H_{\text{rxn}} = -29 \text{ kcal/mol}$). Subsequent tautomerization results in the formation of the respective dibromophenols ($\Delta H_{\text{rxn}} = -17 \text{ kcal/mol}$) (33). The dibromophenols were also detected in our previous study of 2-MBP under pyrolytic conditions (14). However, they were observed over a narrower temperature range and lower yields (14).

On the basis of our pseudo-equilibrium calculations at 700 °C, the concentrations of Br₂ ($9.4 \times 10^{-6} \text{ mol}$) and Br[•] ($9.6 \times 10^{-7} \text{ mol}$) are, respectively, 3 and 1 orders of magnitude higher than the concentration of HBr ($5.4 \times 10^{-8} \text{ mol}$). This

SCHEME 1. Reaction Mechanism for the Formation of 2,4-Dibromophenol and 2,6-Dibromophenol from 2-Bromophenoxy Radical



is in contrast to the results for 2-MCP, where the concentration of HCl (1.7×10^{-5} mol) was greater than that of Cl_2 (1.3×10^{-6} mol) and Cl^\bullet (1.5×10^{-7} mol) (22) and our calculations for the pyrolysis of 2-MBP for which the HBr, Br_2 , and Br^\bullet concentrations were 4.2×10^{-7} , 2.0×10^{-12} , and 2.7×10^{-10} mol, respectively. The addition of oxygen creates $\bullet\text{OH}$, which converts HBr into water and Br^\bullet , the latter being in equilibrium with Br_2 (28). The increased yield of brominated products under oxidative conditions is likely due to the release of strong brominating agents, Br^\bullet , as well as the increase in bromophenoxy radical concentration.

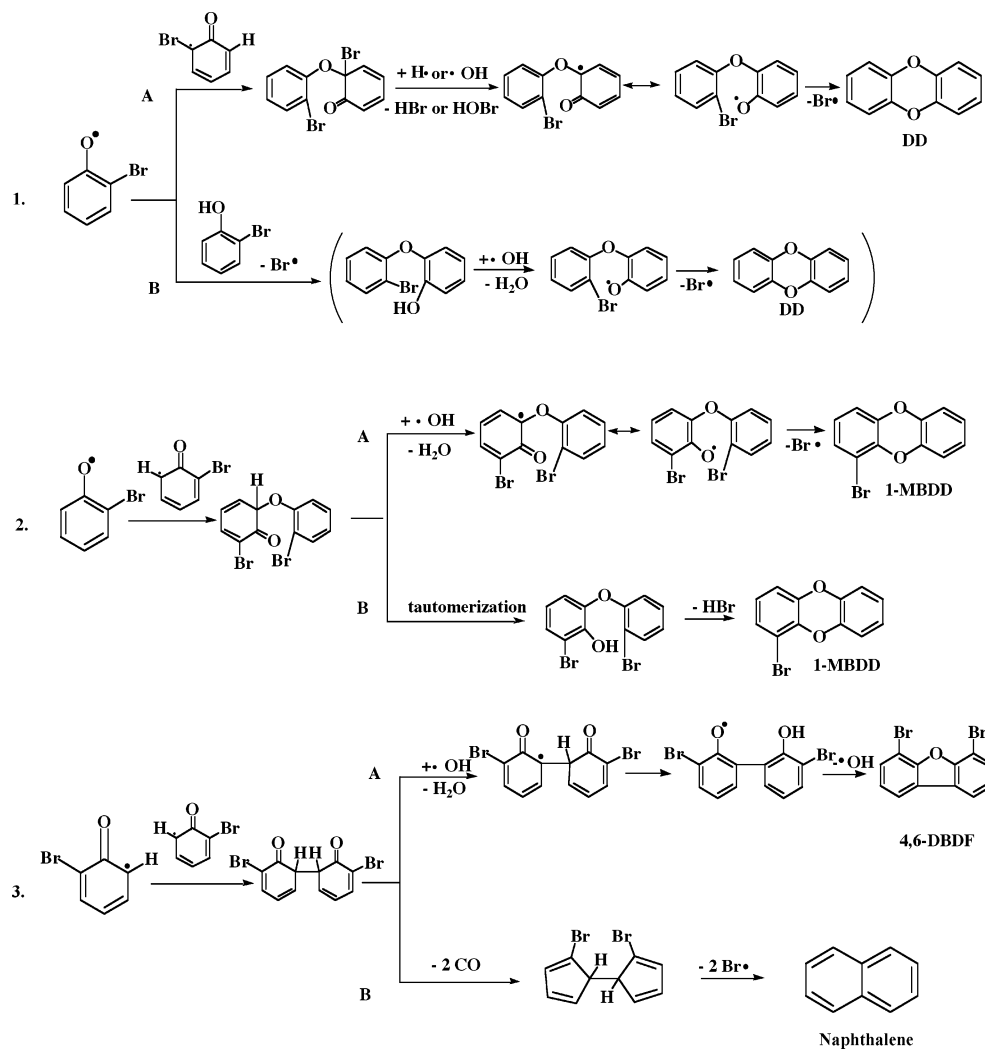
Formation of Naphthalene and Bromonaphthalene.

Formation of polycyclics such as naphthalene and bro-

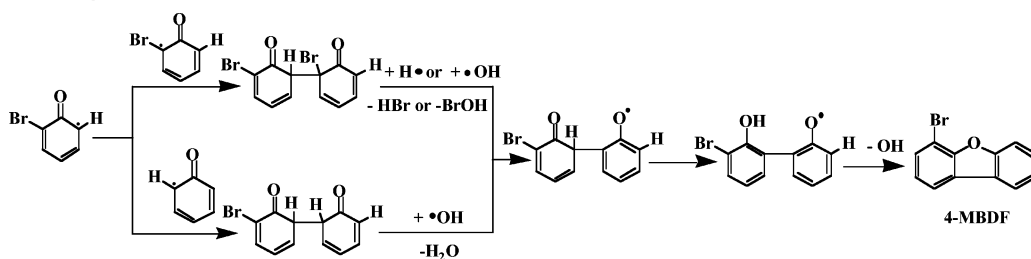
monaphthalene has been traditionally ascribed to molecular growth pathways involving largely C2 fragments (30–32). However, the low-temperature onset of formation of naphthalene (400 °C) suggests a pathway that does not require the complete fragmentation of 2-MBP. In our previous work on the pyrolysis of 2-MBP we presented a reasonable pathway for the formation of naphthalene from the 2-bromophenoxy radical through elimination of CO to form a cyclopentadienyl radical (14). The recombination of two cyclopentadienyl radicals has been previously shown to be a favorable pathway for formation of naphthalene (34, 35). A similar low-temperature route to the formation of naphthalene from the recombination of bromophenoxy radicals is described in Scheme 2 (vide infra) as a competitive pathway to the formation of 4,6-DBDF. This formation of naphthalene is based on a previously proposed pathway of the recombination of two chlorophenoxy radicals to form naphthalene (36).

The yields of naphthalene and bromonaphthalene are significantly lower under oxidative than pyrolytic conditions, most probably due to the more rapid rate of oxidation of the cyclopentadienyl radical (14). Also, with the increase in the concentration of brominated phenoxy radicals, the rate of PBDD/F formation will increase in competition with elimination of CO. The oxidation rate of naphthalene is also increased. Thus, the concentration of naphthalene is dramatically lowered and never becomes a major product as it did under pyrolytic conditions.

SCHEME 2. Pathways for Formation of DD, 1-MBDD, and 4,6-DBDF



SCHEME 3. Pathways for the Formation of 4-MBDF



The formation of naphthalene for the oxidation of both 2-MCP and 2-MBP occurred over a similar temperature range. However, higher yields of naphthalene were observed for the oxidation of 2-MCP than for 2-MBP (22). This may be due to the higher concentration of bromophenoxy than chlorophenoxy radicals, leading to an increased rate of formation of PBDD/F by radical recombination processes at the expense of CO elimination, leading to naphthalene formation.

Formation of Dibenzo-*p*-dioxin, 1-Bromodibenzo-*p*-dioxin, 4,6-Dibromodibenzofuran, 4-Bromodibenzofuran, and Dibenzofuran. Scheme 2 summarizes previously identified reaction pathways to DD, 1-MBDD, and 4,6-DBDF from reaction of the different mesomers of 2-bromophenoxy radical.

Pathway 1a in Scheme 2 depicts the mechanism for DD formation; the oxygen-centered radical mesomer recombines with the carbon- (bromine substituted) centered radical mesomer to form a keto-ether. Following abstraction of bromine by H[•] or [•]OH, DD is formed by intra-annular elimination of Br[•]. Another possible pathway for the formation of DD is through a radical-molecule reaction, pathways 1b, shown in parentheses below the radical-radical pathway in Scheme 2. This reaction depicts the oxygen-centered radical mesomer reacting with 2-MBP via Br[•] displacement to form a bromohydroxy diphenyl ether (HDE) followed by abstraction of hydrogen by [•]OH. Finally, DD is formed by intra-annular displacement of Br[•]. It has been previously suggested that this radical-molecule reaction is too slow to account for the observed yields of the DD (37–39).

Formation of 1-MBDD, shown as pathway 2a in Scheme 2, is initiated by recombination of the oxygen-centered radical mesomer and the carbon (hydrogen)-centered radical mesomer to form a keto-ether. Following loss of hydrogen to form the phenoxy phenyl ether (PPE), ring closure to form 1-MBDD occurs through intra-annular displacement of Br[•]. Pathway 2b depicts an alternate unimolecular pathway for the formation of 1-MBDD.

Pathway 3a depicts a possible pathway to 4,6-DBDF formation. Initially, for both pathways 3a and 3b two carbon-hydrogen-centered radical mesomers react to give the diketo dimer. The dimer can follow the upper pathway, 3a, by abstraction of hydrogen by [•]OH and then undergo tautomerization followed by displacement of [•]OH to form 4,6-DBDF. Pathway 3b is the alternative pathway to formation of naphthalene through CO and Br[•] elimination (36).

We believe that DF is simply a recombination of unbrominated phenoxy radical formed from decomposition of phenol (40). The reaction proceeds by mechanisms analogous to those shown for formation of 4,6-DBDF in Scheme 2.

Scheme 3 depicts proposed pathways for the formation of 4-MBDF. Two pathways are depicted: (1) the carbon (hydrogen)-centered radical mesomer recombines with the carbon (bromine)-centered radical mesomer or (2) the carbon (hydrogen)-centered radical mesomer recombines with an unbrominated carbon-centered phenoxy radical to form a diketo dimer. For the first pathway H[•] abstracts bromine, and in the second [•]OH abstracts another hydrogen. Both

pathways then undergo tautomerization followed by displacement of hydroxyl to form 4-MBDF. Under oxidative conditions the latter pathway is more favorable, while under pyrolytic conditions the former is dominant.

Oxidation versus Pyrolysis of 2-MBP. DD is the major product of both pyrolysis and oxidation of 2-MBP. However, the yield of DD is 4 times greater for oxidation than for pyrolysis (14). This is primarily due to the increase in bromophenoxy radicals at lower temperatures for oxidative conditions, which react to form PBDD/Fs. Under pyrolytic conditions bromophenoxy radicals form at higher temperatures, where their rate of decomposition is greater and yields of PBDD/F are reduced. The yield of 1-MBDD is 5× greater under oxidative conditions than pyrolytic conditions. Its formation is again facilitated by the increase in bromophenoxy radicals. However, the presence of [•]OH facilitates hydrogen abstraction in pathway 2a, which further promotes formation of 1-MBDD.

Detection of 1-MBDD is also observed as low as 400 °C. This is a dramatically lower than the 650 °C formation temperature observed under pyrolytic conditions (14). This suggests another pathway is involved in the low-temperature formation. In our previous study of the oxidation of 2-MCP similar results were observed where 1-MCDD was detected as low as 400 °C (22). We suggested that at lower temperatures 1-MCDD can be formed by a unimolecular pathway following the formation of the keto-ether intermediate via radical-radical recombination. An analogous pathway is proposed for formation of 1-MBDD (cf. pathway 2a in Scheme 2). Alternately to the abstraction of hydrogen by [•]OH in pathway 2a in Scheme 2, a simple, intra-ring, single-proton tautomerization results in the formation of a hydroxyl-diphenyl ether intermediate that can then form 1-MBDD by inter-ring elimination of HBr. This proposed mechanism is based on the similar observation of naphthalene at temperatures as low as 400 °C. Previous work has proposed that after recombination of chlorinated phenoxy radicals to form the diketo intermediate, the formation of naphthalene shown in pathway 3b in Scheme 2 is unimolecular (39). Following recombination the resulting intermediate eliminates two CO moieties, resulting in the formation of bicyclopentadienyl. On the basis of their similarity to the chlorophenoxy radicals, naphthalene can be formed by the bromophenoxy radicals in a similar manner. Naphthalene is then formed by the rearrangement pathways previously proposed in the literature (14, 34, 35). Once the diketo intermediate is formed, the entire process is unimolecular. This can explain the high yields at low temperatures before the radical pool has developed. However, above 500 °C the radical pool increases rapidly and bimolecular pathways involving H[•] and Br[•] abstraction begin to dominate the formation of 1-MBDD and other PBDD/F products. The formation of DD and 4-MBDF at 400–450 °C is attributed to the lower temperature formation of the bromophenoxy radical precursor.

One product not observed under pyrolytic conditions, 4,6-DBDF, was detected in high yields under oxidative conditions (14). This behavior is similar to that observed for 2-MCP (22). With the addition of oxygen, [•]OH becomes the

major carrier over H[•]. Hydroxyl radical facilitates highly exothermic hydrogen-abstraction reactions in pathways 2a (−46 kcal/mol) and 3a (−47 kcal/mol), resulting in the formation of 1-MBDD and 4,6-DBDF, respectively. However, the abstraction of bromine by •OH is 40 kcal/mol endothermic and not favorable. Thus, the increase in •OH concentration increases the rate of 1-MBDD and 4,6-DBDF formation but does not increase the rate of DD formation, which requires abstraction of bromine.

However, 4,6-DBDF is not the major PBDD/F product like 4,6-DCDF is for the analogous oxidation of 2-MCP (22). In the competing pathway to formation of DD from 2-MBP or 2-MCP, the final ring closure involves elimination of Br[•] or Cl[•], respectively. For 2-MBP this step is 12 kcal/mol exothermic, while it is 12 kcal/mol endothermic for 2-MCP. The addition of •OH to the system increases the rates of formation of both 4,6-DBDF and 4,6-DCDF by promoting hydrogen abstraction in pathway 3a. However, this increase is insufficient to dominate over the exothermic formation of DD from 2-MBP, whereas it is sufficient to compete with the endothermic formation of DD from 2-MCP (14). Therefore, DD remains the dominant PBDD/F product for 2-MBP.

The yields of 4,6-DBDF and 1-MBDD are ~5× less than the yields of 4,6-DCDF and 1-MCDD. This may be due to the more exothermic abstraction of hydrogen by •OH by 12 kcal/mol for the chlorinated reaction intermediates than the corresponding brominated intermediates as well as the 28 kcal/mol more exothermic abstraction of hydrogen by Cl[•] than hydrogen by Br[•]. On the basis of our pseudo-equilibrium calculations for 2-MBP and similar calculation for the 2-MCP system, the addition of oxygen to the system increases the concentrations of •OH and Br[•]. However, the hydrogen-abstraction reactions necessary for formation of 4,6-DBDF and 1-MBDD from 2-MBP are not as favored by this increase as in the 2-MCP system.

The maximum yield of 4-MBDF is 16 times higher under oxidative conditions than pyrolysis (14). This can be explained in the same way as the formation of 4,6-DBDF is explained. With the addition of oxygen, the lower pathway in Scheme 3 is the more favorable pathway in that the addition of •OH will lower ΔH_{rxn} for the abstraction of hydrogen (−47 kcal/mol) by 17 kcal/mol over the abstraction of hydrogen by H[•]. The upper pathway in Scheme 3, the abstraction of bromine by •OH, is endothermic by 35 kcal/mol. Thus, the upper pathway is not affected by the addition of oxygen other than with the increase in bromophenoxy radicals.

In summary, we proposed reasonable mechanisms for the formation of each observed product of the oxidation of 2-MBP. We also identified mechanistic rationales for the differences in product distribution and PBDD to PBDF branching ratios for oxidative versus pyrolytic conditions. Comparison of oxidation and pyrolysis results has also identified possible lower temperature, primarily unimolecular routes to formation of naphthalene and 1-MBDD that can occur before the radical pool increases significantly at 600 °C. On the basis of a comparison of the oxidation of 2-MBP and 2-MCP, there is a 20× greater yield of DD formation for 2-MBP (22). This indicates the increased propensity for dioxin formation from brominated precursors. Thus, the presence of brominated flame retardants in incinerators and energy-recovery devices as well as accidental fires suggests that additional attention should be paid to PBDD/F formation from combustion of brominated chemicals and materials.

Acknowledgments

We gratefully acknowledge the assistance of our colleagues, Dr. Lavrent Khachatryan and Alexander Burcat, in evaluation of the thermochemistry presented in this manuscript as well as helpful discussions concerning the mechanisms of dioxin formation. We acknowledge the partial support of this work

under EPA Contract 9C-R369-NAEX, EPA Grant R828166, and the Patrick F. Taylor Chair foundation.

Literature Cited

- de Wit, C. An Overview of Brominated Flame Retardants in the Environment. *Chemosphere* **2002**, *46*, 583.
- Soderstrom, G.; Marklund, S. PBDD and PBCDF from Incineration of Waste-Containing Brominated Flame Retardants. *Environ. Sci. Technol.* **2002**, *36*, 1959.
- Thoma, H.; Rist, S.; Haushulz, G.; Hutzinger, O. Polybrominated Dibenzodioxins and -furans from the Pyrolysis of Some Flame Retardants. *Chemosphere* **1986**, *15* (4), 649.
- Oberg, T.; Warman, K.; Bergstrom, S. Brominated Aromatics in Combustion. *Chemosphere* **1987**, *16*, 2451.
- Dumlar, R.; Thoma, H.; Lenoir, D.; Hutzinger, O. PBDF and PBDD from the Combustion of Bromine Containing Flame Retarded Polymers: A Survey. *Chemosphere* **1989**, *19* (12), 2023.
- Sakai, S. Thermal Behavior of Brominated Flame Retardants and PBDDs/DFs. *Organohalogen Compd.* **2000**, *47*, 210.
- Sakai, S.; Watanabe, J.; Honda, Y.; Takatsuku, H.; Aoki, I.; Futamatsu, M.; Shiozaki, K. Combustion of Brominated Flame Retardants and Behavior of its Byproducts. *Chemosphere* **2001**, *42*, 519.
- Wilken, M.; Schanne, L. Brominated Dioxins—A Potentially Greater Hazard in Fires than PCDD and PCDF? *Schriftenreihe WAR* **1994**, *74*, 109.
- Lemieux, P. M.; Ryan, J. V. Enhanced Formation of Dioxins and Furans from Combustion Devices by Addition of Trace Quantities of Bromine. *Waste Manage.* **1998**, *18*, 361.
- Kanters, J.; Louw, R. Thermal and Catalysed Halogenation in Combustion Reactions. *Chemosphere* **1996**, *32* (1), 87.
- Buser, H. R. Polybrominated Dibenzofurans and Dibenzodioxins: Thermal Reaction Products of Polybrominated Diphenyl Ether Flame Retardants. *Environ. Sci. Technol.* **1986**, *20*, 404.
- Dumlar, R.; Thoma, H.; Lenoir, D.; Hutzinger, O. Thermal Formation of Polybrominated Dibenzodioxins (PBDD) and Dibenzofurans (PBDF) from Bromine Containing Flame Retardants. *Chemosphere* **1989**, *19* (1–6), 305.
- Sidhu, S. S.; Maqsd, L.; Dellinger, B. The Homogeneous, Gas-Phase Formation of Chlorinated and Brominated Dibenzodioxins from 2,4,6-Trichlorophenol and 2,4,6-Tribromophenols. *Combust. Flame* **1995**, *100*, 11.
- Evans, C.; Dellinger, B. Mechanisms of Dioxin Formation from the High-Temperature Pyrolysis of 2-Bromophenol. *Environ. Sci. Technol.* **2003**, *37*, 5574.
- Menear, J. H.; Lee, C. C. Polybrominated Dibenzodioxins and Dibenzofurans: Literature Review and Health Assessment. *Environ. Health Perspect.* **1994**, *102* (1), 265.
- Weber, L. W.; Greim, H. The Toxicology of Brominated and Mixed-Halogenated Dibenzodioxins and Dibenzofurans: An Overview. *J. Toxicol. Environ. Health* **1997**, *50* (3), 195.
- Wiater-Protas, I.; Louw, R. Gas-Phase Chemistry of Chlorinated Phenols—Formation of Dibenzofurans and Dibenzodioxins in Slow Combustions. *Eur. J. Org. Chem.* **2001**, 3945.
- Born, J. G. P.; Louw, R.; Mulder, P. Formation of Dibenzodioxins and Dibenzofurans in Homogeneous Gas-Phase Reactions of Phenols. *Chemosphere* **1989**, *19*, 401.
- Weber, R.; Hagenmaier, H. Mechanism of the Formation of Polychlorinated Dibenzodioxins and Dibenzofurans from Chlorophenols in Gas-Phase Reactions. *Chemosphere* **1999**, *38*, 529.
- Weber, R.; Hagenmaier, H. On the Mechanism of the Formation of Polychlorinated Dibenzofurans from Chlorophenols. *Organohalogen Compd.* **1997**, *31*, 480.
- Evans, C. S.; Dellinger, B. Mechanisms of Dioxin Formation from the High-Temperature Pyrolysis of 2-Chlorophenol. *Environ. Sci. Technol.* **2003**, *37*, 1325.
- Evans, C. S.; Dellinger, B. Mechanisms of Dioxin Formation from the High-Temperature Oxidation of 2-Chlorophenol. *Environ. Sci. Technol.* **2005**, *39*, in press.
- Rubey, W. A.; Grant, R. A. Design Aspects of a Modular Instrumentation System for Thermal Diagnostic Studies. *Rev. Sci. Instrum.* **1988**, *59*, 265.
- ChemBats3D Pro*, version 8.0; CambridgeSoft Corp.: Cambridge, MA, 2003.
- Chemkin*, version 3.6; Reaction Design, Inc.: San Diego, CA, 2002.
- Shaub, W. M.; Tsang, W. Dioxin Formation in Incinerators. *Environ. Sci. Technol.* **1983**, *17*, 721.

- (27) Colussi, A.; Zabel, F.; Benson, S. W. The Very Low-Pressure Pyrolysis of Phenyl Ethyl Ether, Phenyl Allyl Ether and Benzyl Methyl Ether and the Enthalpy of Formation of the Phenoxy Radical. *Int. J. Chem. Kinet.* **1977**, *9*, 161.
- (28) *NIST Chemical Kinetics Database 17*; NIST: Gaithersburg, MD, 1998.
- (29) McMillen, D. F.; Golden, D. M. Hydrogen Bond Dissociation Energies. *Annu. Rev. Phys. Chem.* **1982**, *33*, 493–532.
- (30) Appel, J.; Bockhorn, H.; Frenklach, M. Kinetic Modeling of Soot Formation with Detailed Chemistry and Physics: Laminar Premixed Flames of C2 Hydrocarbons. *Combust. Flame* **2000**, *121*, 122.
- (31) Richter, H.; Howard, J. B. Formation of Polycyclic Aromatic Hydrocarbons and Their Growth to Soot—A Review of Chemical Reaction Pathways. *Prog. Energy Combust. Sci.* **2000**, *26*, 4.
- (32) Richter, H.; Mazzer, O. A.; Sumathi, R.; Green, W. H.; Howard, J. A.; Bozzelli, J. W. Detailed Kinetic Study of the Growth of Small Polycyclic Aromatic Hydrocarbons, 1. 1-Naphthyl + Ethyne. *J. Phys. Chem. A* **2001**, *105* (9), 1561.
- (33) Capponi, M.; Gut, I.; Hellrum, B.; Persy, G.; Wirz, J. Ketonization Equilibria of Phenol in Aqueous Solution. *Can. J. Chem.* **1999**, *77*, 605.
- (34) Melius, C. F.; Calvin, M.; Marinov, N. M.; Ritz, W. J.; Senkan, S. M. Reaction Mechanisms in Aromatic Hydrocarbon Formation Involving the C₅H₅ Cyclopentadienyl Moiety. *26th Symposium (International) on Combustion*; The Combustion Institute: Pittsburgh, 1996; p 685.
- (35) Lu, M.; Mulholland, J. A.; Aromatic Hydrocarbon Growth from Indene. *Chemosphere* **2001**, *42*, 623.
- (36) Kim, D. H.; Mulholland, J. A.; Ryu, J.-Y. Formation of Polychlorinated Naphthalenes from Chlorophenols. *26th Symposium (International) on Combustion*; The Combustion Institute: Pittsburgh, in press.
- (37) Khachtrayan, L.; Burcat, A.; Dellinger, B. An Elementary Reaction-Kinetic Model for the Gas-Phase Formation of 1,3,6,8- and 1,3,7,9-Tetrachlorinated Dibenzo-p-dioxins from 2,4,6-Trichlorophenol. *Combust. Flame* **2003**, *132*, 406.
- (38) Khachtrayan, L.; Asatryan, R.; Dellinger, B. Development of Expanded and Core Kinetic Models for the Gas Phase Formation of Dioxins from Chlorinated Phenols. *Chemosphere* **2003**, *52*, 695.
- (39) Louw, R.; Ahonkhai, S. T. Radical/radical vs Radical/molecule Reactions in the Formation of PCDD/Fs from (Chloro)phenols in Incinerators. *Chemosphere* **2002**, *46*, 1273.
- (40) Wiater, I.; Born, J. G. P.; Louw, R. Products, Rates and Mechanism of the Gas-Phase Condensation of Phenoxy Radicals between 500–840 K. *Eur. J. Org. Chem.* **2000**, 921.

Received for review September 29, 2004. Revised manuscript received December 28, 2004. Accepted January 11, 2005.

ES048461Y